Original Article

The circular RNA circ_0099630/miR-940/receptor-associated factor 6 regulation cascade modulates the pathogenesis of periodontitis

Xue-Qin Zhao, Chuan-Bei Ao*, Yi-Tong Yan

Department of Stomatology, Stomatological Hospital of Jingmen Second People's Hospital, Jingmen, China

Abstract *Background/purpose:* Periodontitis is one of the highly prevalent chronic inflammatory conditions in adults. The importance of circular RNAs (circRNAs) in the regulation of inflammation has been gradually reported in recent years, but the role of circRNA circ_0099630 in periodontitis has not been reported.

Materials and methods: The contents of circ_0099630, microRNA-940 (miR-940) and tumor necrosis factor (TNF) receptor-associated factor 6 (TRAF6) were measured using quantitative real-time polymerase chain reaction (qRT-PCR) or Western blot. Inflammatory factor secretion, cell proliferation, and apoptosis were analyzed under the application of Enzyme-linked immunosorbent assay (ELISA), Cell Counting Kit-8 (CCK8), 5-ethynyl-2'-deoxyuridine (EdU) and flow cytometry, respectively. The Western blot also analyzed the phosphorylation levels of RELA proto-oncogene (P65) and IkappaBalpha (IκBα), key molecules of the nuclear factor kappa-B (NF-κB) pathway. The relationship between miR-940 and circ_0099630 or TRAF6 was verified by luciferase reporter system and RNA immunoprecipitation (RIP) assay.

Results: Higher abundance of circ_0099630 and TRAF6 and lower miR-940 expression were observed in periodontitis, and circ_0099630 knockdown attenuated the damage of human PDL cells (PDLCs) induced by lipopolysaccharides (LPS). The relationship between miR-940 and circ_0099630 or TRAF6 was evidenced, while miR-940 downregulation diminished the

repair effect of si-circ_0099630 on overexpression LPS-induced damage in PDLCs. Similarly, TRAF6 upregulation impaired the mitigating effect of miR-940 overexpression on LPS-induced injury in PDLCs. Circ_0099630 silencing evidently curbed the phosphorylation levels of P65 and IκBα and thus attenuating the inflammatory response by acting on the miR-940/TRAF6 axis.

Conclusion: Silencing circ_0099630 alleviates LPS-induced periodontal ligament cell injury via targeting miR-940/TRAF6/NF-κB in periodontitis.

Introduction

Periodontitis is a complex infectious disease that occurs mostly in early adulthood and is reflected in pathological changes in the periodontal ligament and alveolar bone.[1] Periodontitis is usually caused by infections such as herpes virus, *aggregatibacter actinomycetemcomitans* and *porphyromonas gingivalis*, and it interacts with the immune system of the body.[2] Periodontitis can be divided into resting periodontitis, which contains a large number of latent herpes viruses,[3] and active periodontitis, in which these viruses are activated, which in turn causes pathogenic bacterial overgrowth and immunosuppression to develop.[4] In addition, activated herpes viruses can promote the progression of gingivitis to periodontitis. The diagnosis of periodontitis is an ongoing clinical challenge, usually accompanied by under- or over-diagnosis, with over-diagnosis being relatively frequent.[5] Therefore, a rapid and accurate diagnosis of periodontitis is now a priority. The treatment of mild periodontitis usually does not require surgical treatment, and the elimination of pathogenic bacteria and calculus by using antibacterial drugs combined with ultrasonic therapy can effectively suppress the number of pathogenic bacteria.[6] Severe periodontitis is usually treated surgically in combination with antibiotic application, but the high cost of surgical treatment and the phenomenon of small treatment differences with antibiotic treatment are the reasons why surgical treatment is not commonly used today.[7] Therefore, it is more urgent to find new ways of diagnosing and treating periodontitis.

Circular RNAs (circRNAs) are a common class of closed-loop RNA molecules among non-coding RNAs.[8] CircRNAs are demonstrated to competitively binding microRNAs (miRNAs) to play regulatory roles by acting as competing endogenous RNAs (ceRNAs). A great number of circRNAs have been identified to be dysregulated in various types of diseases.[9—12] In cancer, numerous circRNAs have been observed to be dysregulated. For instance, circRNA CDR1 antisense RNA (Cdr1as) was revealed to be abnormally upregulated in hepatocellular carcinoma (HCC) cells, and circRNA Cdr1as upregulation acting on the miR-1270/alpha fetoprotein (AFP) axis accelerated the proliferation and metastasis of hepatocellular carcinoma cells, which revealed that circRNA Cdr1as had the promise to become a molecular marker for HCC diagnosis.[9] CircRNAs were also demonstrated to play a role in preeclampsia (PE), a multi-system disorder. For example, circ_0003496 was less abundant in placental tissues and acted on the miR-1244/forkhead box M1 (FOXM1) axis to regulate PE progression.[10] This indicated that circ_0003496 might be a future molecular marker in the diagnostic and therapeutic process of PE. Further, dysregulation of circRNAs was also found in various types of inflammatory diseases. Zhang et al. established that circ_0005567 competitively bound miR-495 to regulate autophagy related 14 (ATG14) level and thus modulated osteoarthritis (OA) progression.[11] Circ_0005567 upregulation attenuated apoptosis in OA model cells, while circ_0005567 knockdown did the opposite.[11] In periodontitis, using RNA sequencing analysis of periodontitis tissues and normal tissues, 1304 differentially expressed circRNAs were found.[12] Among these circRNAs, circ_0138960 was confirmed to be greatly upregulated in periodontitis tissues,[12] but no validation of the mechanism was performed. Herein, our study explored the role and mechanism of circ_0099630 in periodontitis.

MiRNAs are a class of tiny RNAs with fragment lengths of 18—25 nt and are members of regulatory non-coding RNAs.[13] MiRNAs are synthesized by different mechanisms in plants and animals and can play a regulatory role by acting on the 3′ untranslated regions (3′UTRs) of target genes to inhibit the initiation and progression of translation.[14] MiRNAs not only play a role in physiological processes such as cell growth and differentiation and death in the body, but have also been identified to be aberrantly expressed in diseases such as cancer, neurological disorders, and inflammation.[15—18] In periodontitis, miR-21 was demonstrated to repress inflammatory responses both *in vitro* and *in vivo* and had potential as a target for periodontitis treatment.[17] Guo et al. demonstrated that miR-218 oppressed the inflammatory response of periodontitis cells by targeting Mmp9.[18] MiR-940 was found to be dysregulated in multiple human diseases.[19,20] For instance, miR-940 upregulation contributed to the proliferation and invasion of breast cancer cells.[19] Conversely, in esophageal squamous cell carcinoma, miR-940 might function as an anti-tumor agent by repressing cell growth and enhancing apoptosis.[21] MiR-940 was also demonstrated to be downregulated in mice with spinal cord injury (SCI), and upregulation of miR-940 restrained the levels of inflammatory factors toll like receptor 4 (TLR4) and myeloperoxidase (MPO), thereby suppressing the inflammatory response and promoting SCI recovery.[20] However, no studies showed whether miR-940 was involved in the pathogenesis of periodontitis. We therefore analyzed the regulatory mechanism of miR-940 in periodontitis.

Tumor necrosis factor receptor-associated factor 6 (TRAF6) is a member of the TRAFs family, which currently has seven members characterized by the C-terminal TRAF domain.[22] TRAF6 was first cloned by Ishida in 1996, and it was demonstrated that upregulation of TRAF6 activated NFkappaB and that TRAF6 mediated CD40 signaling to regulate B-cell function.[23] It was demonstrated that TRAF6 had a 530 amino acid composition, was less homologous than other TRAFs family members, and had been detected as expressed in a variety of human tissues.[24] Yuan et al. identified that TRAF6 upregulation was notably associated with apoptosis rates in stroke cell models and also enhanced inflammatory responses.[25] The action mechanism of circ_0099630/miR-940/TRAF6 in periodontitis was investigated in this study.

Materials and methods

Sample collection

Periodontal tissues from 26 patients with periodontitis (9 cases mild, 10 cases moderate and 7 cases severe divided according to the severity of periodontitis) and 21 volunteers without periodontitis were collected from Stomatological Hospital of Jingmen Second People's Hospital, volunteers in both groups were free of other diseases and were not treated with antibiotics for one month prior to sample collection. Sample collection and follow-up tests were approved by Stomatological Hospital of Jingmen Second People's Hospital ethics committee along with informed consent and written confirmation from all participants.

Quantitative real-time polymerase chain reaction

RNA from periodontal ligament (PDL) tissues and cells was extracted with the help of TRIzol (TaKaRa, Dalian, China). Immediately afterwards, reverse transcription (RT) was executed adhering to the instructions of the AMV Reverse Transcriptase (Solarbio, Beijing, China) and miScript RT Kit (TaKaRa). The quantitative real-time polymerase chain reaction (qRT-PCR) with cDNA as template was carried out exactly as described in the SYBR Green (TaKaRa) instructions, and information on the primers used in this procedure was listed in Supplement Table 1. We normalized to the qRT-PCR data by glyceraldehyde-3-phosphate dehydrogenase (GAPDH) and U6 small nuclear RNA (U6).

RNase R treatment

RNA was mixed with $3U/\mu g$ of RNase R (Solarbio) was mixed and co-incubated at 37 °C for 30 min. We analyzed circ_0099630 and GAPDH contents in this RNA with reference to the above steps.

Cell culture and transfection

Human PDL cells (PDLCs) were obtained from the China center for type culture collection (Wuhan, China). PDLCs were grown in Dulbecco's Modified Eagle Medium (DMEM) medium supplemented with 10% fetal bovine serum (FBS) and 1% double antibodies and were placed at 37 °C in 5% CO_2. Subsequently, PDLCs were induced by 0 μg/mL, 2 μg/mL, 4 μg/mL, and 8 μg/mL of lipopolysaccharides (LPS) (Sigma–Aldrich, St. Louis, MO, USA) for 24 h to obtain periodontitis model cells. The circ_0099630 small interfering RNA (si-circ_0099630) and negative control (si-NC), miR-940 mimic (miR-940), miR-940 inhibitor (anti-miR-940) and negative controls (miR-NC, anti-miR-NC), TRAF6 overexpression vector (TRAF6) and negative control (pcDNA) all from Songon (Shanghai, China) were transfected into PDLCs following the Lipofectamine 2000 (Invitrogen, Carlsbad, CA, USA) guidelines.

Enzyme-linked immunosorbent assay

Cellular levels of interleukin-6 (IL-6) and tumor necrosis factor-α (TNF-α) were assessed by enzyme-linked immunosorbent assay (ELISA) following the instructions of the corresponding ELISA kits (Beyotime, Shanghai, China). Cells were first lysed, then the supernatant of the lysate was incubated with detection reagents protected from light, and finally an enzyme marker was used for quantitative analysis.

Cell Counting Kit-8 assay

Cell viability of PDLCs was estimated by Cell Counting Kit-8 (CCK8) assay and the whole procedure was carried out following the instructions of Cell Counting Kit-8 (Beyotime). 96-well plates of PDLCs were incubated with 10 μL of CCK8 solution 24 h after transfection and then the absorbance at 450 nm was measured.

5-Ethynyl-2′-deoxyuridine assay

The proliferation of PDLCs was analyzed by 5-ethynyl-2′-deoxyuridine (EdU) assay accompanied by the use of the EdU Cell Proliferation Assay Kit (Beyotime). PDLCs were inoculated in 96-well plates for 24 h. PDLCs were first labeled with 10 μL EdU. After the cells were washed with PBS, 100 μL of click reaction solution was added for 30 min, and 20 μL DAPI was applied to the labeled cells for staining, which were then immediately placed under a fluorescent inverted microscope for observation.

Apoptosis assay

Assessment of apoptosis with the Annexin V-fluorescein isothiocyanate (FITC)/propidium iodide (PI) Apoptosis Detection Kit (Solarbio) was done. The digested PDLCs were collected and mixed with binding buffer, 5 μL Annexin V-FITC and PI were added and mixed with the obtained single cell suspensions, placed in the dark for 15 min, and the apoptosis of PDLCs was analyzed using flow cytometry.

Western blot

PDLCs were lysed in the presence of radioimmune precipitation assay (RIPA) buffer (Beyotime), then total protein was captured and the protein was quantified by Bicinchoninic acid (BCA) Protein Assay Kit (Beyotime). Equal amounts of proteins

were utilized for Western blot. After sodium dodecyl sulfate-polyacrylamide gel electrophoresis (SDS-PAGE), the proteins were transferred to polyvinylidene fluoride (PVDF) membranes (Beyotime), and the blocking solution (Beyotime) was mixed with the membranes for 2 h. After that, the membranes were co-incubated with anti-Cleaved-caspase-3 (ab32042, 1:500, Abcam, Cambridge, UK), anti-BCL2 associated X (anti-Bax, ab32503, 1:1000, Abcam), anti-GAPDH (ab8245, 1:1000, Abcam), anti-TRAF6 (ab33915, 1:2000, Abcam), anti-RELA proto-oncogene (anti-P65, ab32536, 1:1000, Abcam), anti-phosphorylated-P65 (anti-p-P65, ab31624, 1:1000, Abcam), anti-IkappaBalpha (anti-IκBα, ab32518, 1:1000, Abcam) and anti-p-IκBα (ab133462, 1:1000, Abcam) at 4 °C overnight. The secondary antibody goat anti-rabbit immunoglobulin G (IgG) (ab205718, 1:20,000, Abcam) was mixed and this membrane on the second day, the proteins were then developed and analyzed in the FluorChem E system (Protein Simple, Silicon Valley, CA, USA).

Dual-luciferase reporter assay

After the target sites of circ_0099630 and miR-940 were predicted by Circinteractome (https://circinteractome.nia.nih.gov/) and Targetscan (http://www.targetscan.org/vert_80/). The wild-type (WT) circ_0099630 and TRAF6 3′UTR sequences containing the miR-940 complementary sites and the mutant (MUT) sequences after mutating the binding sites were cloned. The successfully constructed WT-circ_0099630, MUT-circ_0099630, WT-TRAF6 3′UTR and MUT-TRAF6 3′UTR were then co-transfected into PDLCs with miR-940 mimic. 24 h later, the cells were lysed and the supernatant was collected, and the luciferase activity of each group was measured using Dual-Lucy Assay Kit (Solarbio).

RNA immunoprecipitation assay

The RNA immunoprecipitation (RIP) assay was completely carried out as per the RNA Immunoprecipitation Kit (Sigma−Aldrich) guidelines, PDLCs lysate was gathered after the addition of RIP lysate. Then the lysate was added with magnetic beads coupled to the Argonaute 2 (Ago2) or IgG antibody (Sigma−Aldrich) and subsequently the RNA in the complex on the beads was captured, circ_0099630, miR-940 and TRAF6 levels were detected.

Statistical analysis

For all experiments repeated three times at least, the obtained data were processed by SPSS 19.0 (SPSS Inc., Chicago, IL, USA). Student's t-test or analysis of variance (ANOVA) was employed in this study for the analysis of the differences between groups. P-value < 0.05 was statistically significant.
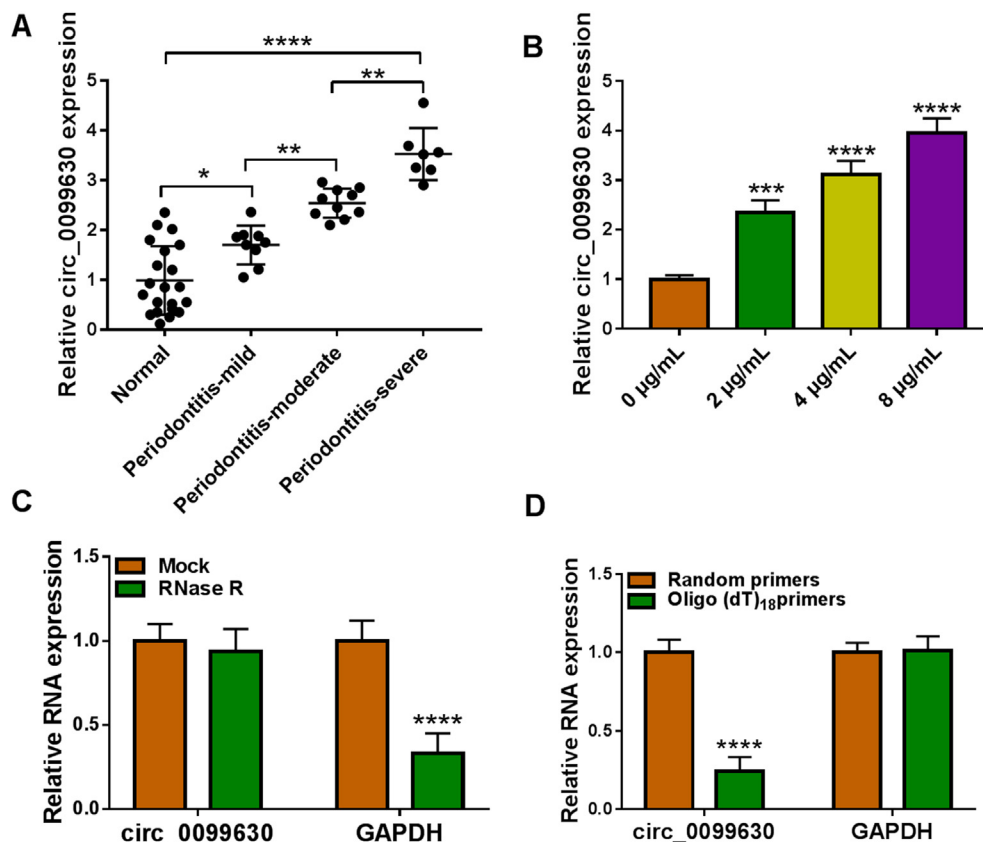

Figure 1   Circ_0099630 level in periodontitis tissues and LPS-induced PDLCs was analyzed. (A and B) Circ_0099630 level was detected in periodontitis tissues and LPS-induced PDLCs by qRT-PCR. (C) The execution of qRT-PCR analyzed the levels of circ_0099630 and GAPDH after RNase R treatment. (D) The amplification effects of Oligo(dt)18 primers and random primers on circ_0099630 and GAPDH were examined using qRT-PCR. *$P < 0.05$, **$P < 0.01$, ***$P < 0.001$, ****$P < 0.001$.

Results

Circ_0099630 abundance was greatly increased in periodontitis tissues and LPS-induced PDLCs

Fig. 1A demonstrated that circ_0099630 content was higher in periodontitis tissues than that in normal tissues, while the expression of circ_0099630 in PDLCs was increased with increasing LPS concentration (Fig. 1B). Moreover, with the progression of the severity of periodontitis, the expression of circ_0099630 was markedly increased (Fig. 1A). We observed essentially no difference in circ_0099630 level before and after RNase R treatment, while GAPDH was substantially degraded after RNase R treatment, strong resistance of circ_0099630 to RNase R was displayed by qRT-PCR results (Fig. 1C). The level of circ_0099630 amplified by Oligo (dT)18 primers was lower than that of circ_0099630 amplified by
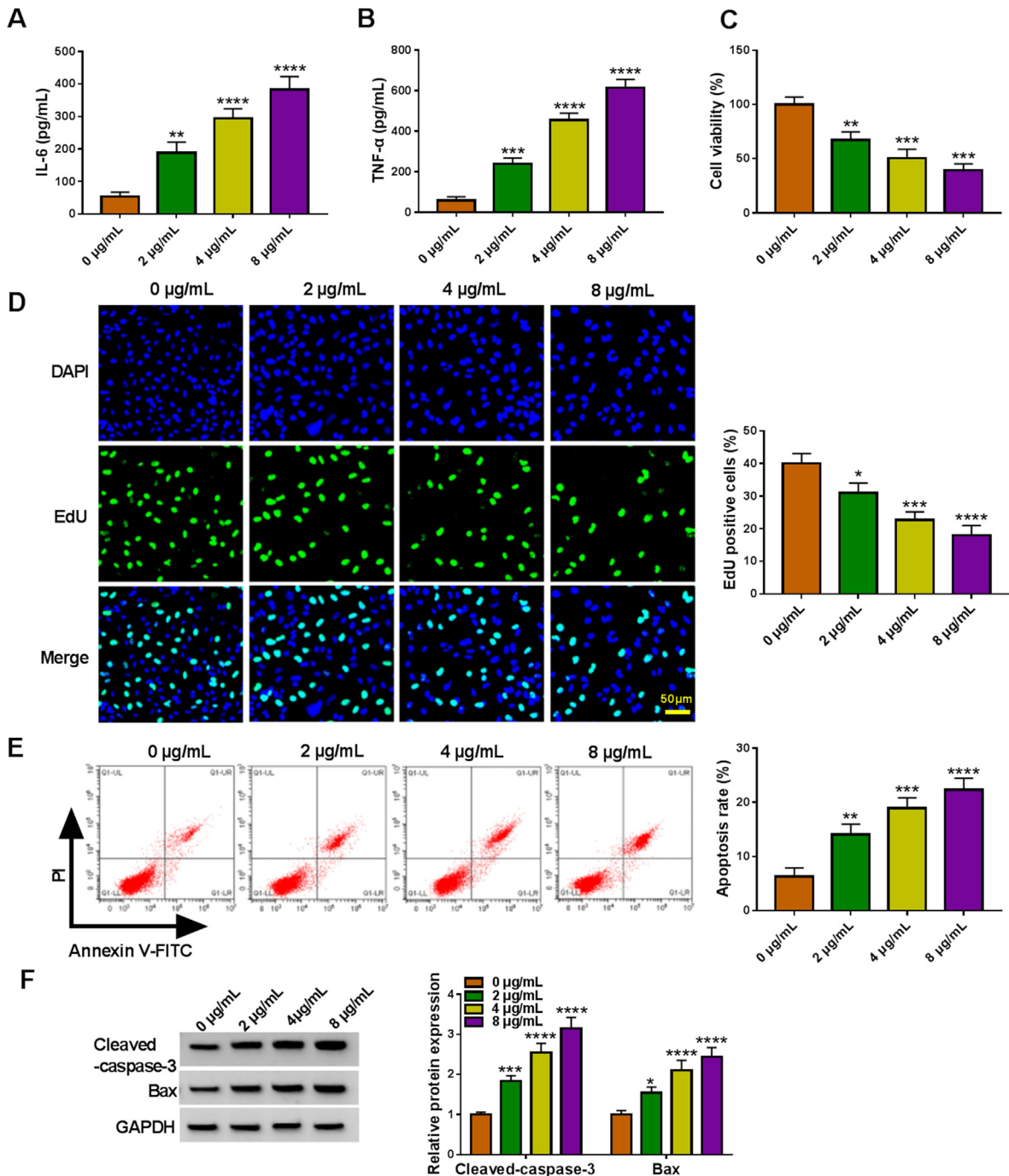

Figure 2 **Effects of different concentrations of LPS on inflammatory response, viability, proliferation and apoptosis of PDLCs.** (A—F) After treatment of PDLCs with 0 μg/mL, 2 μg/mL, 4 μg/mL, and 8 μg/mL of LPS, (A and B) IL-6 and TNF-α levels were measured by ELISA. (C) CCK8 assay measured cell viability. (D) The application of EdU assay assessed cell proliferation. (E) Apoptosis rate was tested by flow cytometry. (F) Cleaved-caspase-3 and Bax levels were measured using Western blot. *$P < 0.05$, **$P < 0.01$, ***$P < 0.001$, ****$P < 0.001$.
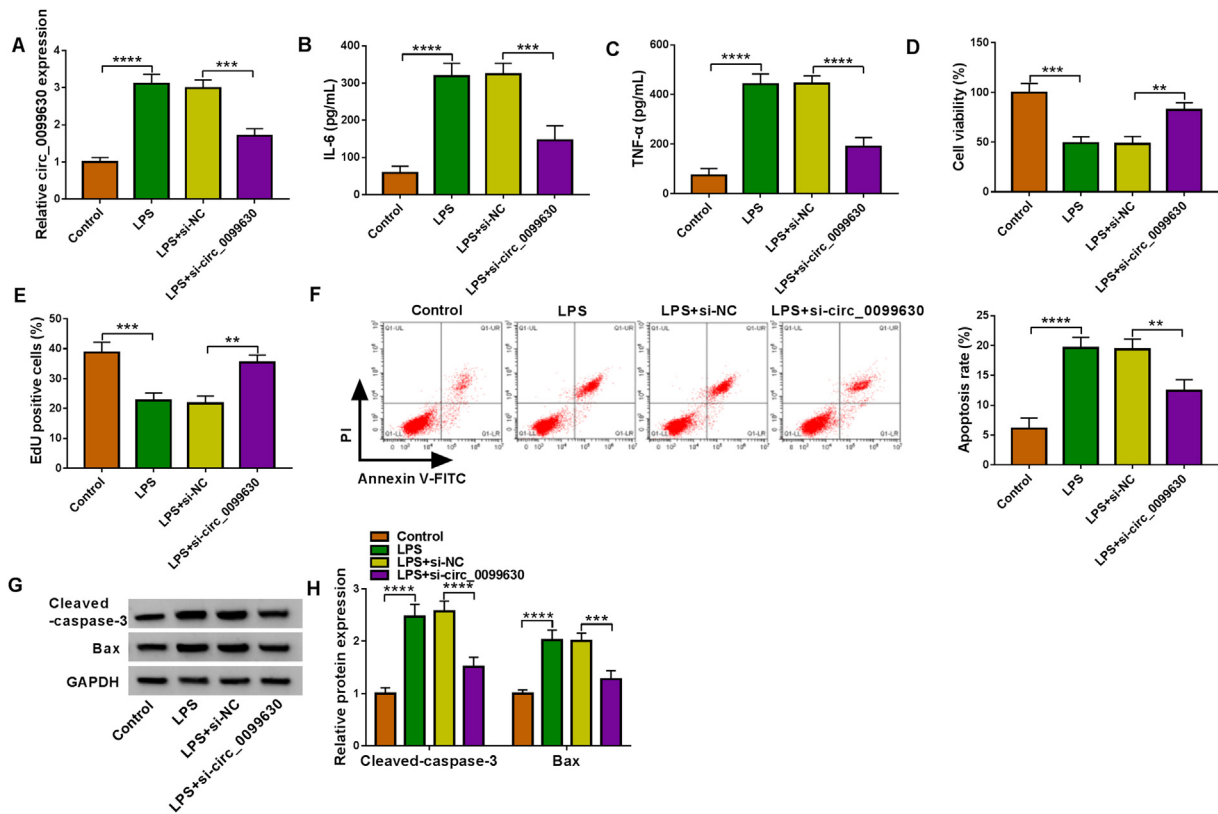
Figure 3 **Effects of circ_0099630 downregulation on LPS-induced PDLCs.** (A—H) The tests were divided into four groups (Control, LPS, LPS + si-NC, LPS + si-circ_0099630). (A) Circ_0099630 level was tested using qRT-PCR. (B and C) Under the use of ELISA, IL-6 and TNF-α cell levels were analyzed. (D) Cell viability was detected by CCK8. (E) EdU was applied to examine proliferation. (F) PDLCs apoptosis was assayed using flow cytometry. (G and H) Cleaved-caspase-3 and Bax protein levels were assessed by Western blot. **$P < 0.01$, ***$P < 0.001$, ****$P < 0.001$.
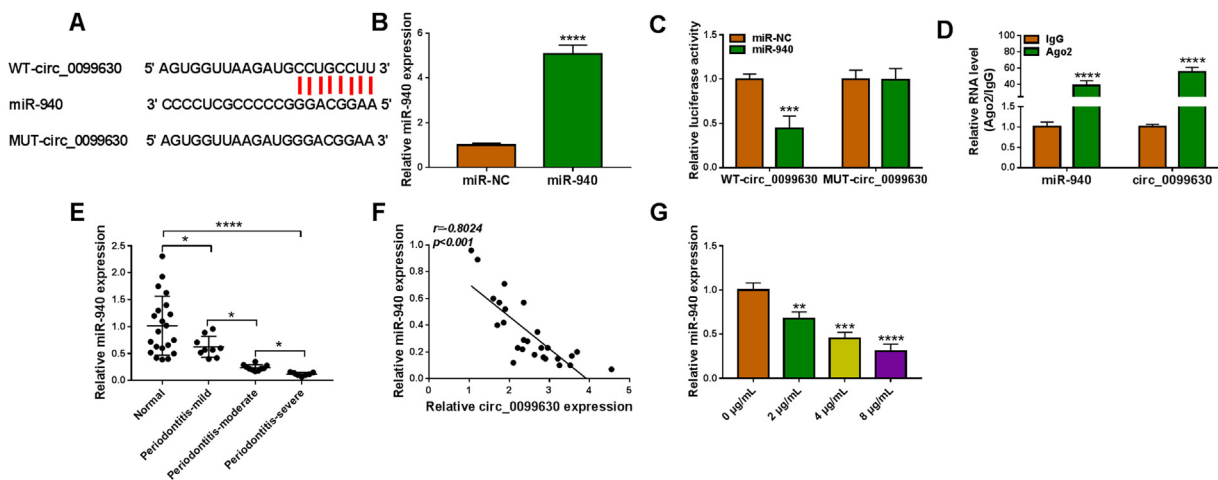

Figure 4 **The relationship between circ_0099630 and miR-940 was evidenced.** (A) The complementary sequences of circ_0099630 and miR-940. (B) Overexpression efficiency of miR-940 mimic was confirmed after the performance of qRT-PCR. (C) Targeting between circ_0099630 and miR-940 was validated using dual-luciferase reporter system. (D) Targeting between circ_0099630 and miR-940 was validated by RIP assay. (E) MiR-940 level in periodontitis tissues was analyzed via qRT-PCR. (F) Pearson's analysis revealed the correlation between miR-940 and circ_0099630 levels in periodontitis tissues. (G) QRT-PCR determined the miR-940 level in LPS-induced PDLCs. *$P < 0.05$, **$P < 0.01$, ***$P < 0.001$, ****$P < 0.001$.

random primers, whereas this difference was not present in the GAPDH group, showing the ring structure feature of circ_0099630 (Fig. 1D). These data suggested that circ_0099630 had higher abundance in periodontitis tissues and LPS-induced PDLCs.

LPS suppressed PDLCs viability, proliferation and enhanced apoptosis and inflammatory response

Cellular levels of inflammatory factors IL-6 and TNF-α were increased with increasing LPS concentration (Fig. 2A and B). The viability and proliferation capacity of PDLCs became progressively weaker with increasing LPS concentration (Fig. 2C and D). Flow cytometry results also confirmed that LPS exhibited a concentration-dependent promotion of apoptosis in PDLCs (Fig. 2E). Protein levels of the apoptosis marker proteins Cleaved-caspase-3 and Bax were promoted with increasing LPS concentration as observed by Western blot (Fig. 2F). Combined with the results of this study, we selected 4 μg/mL of LPS for the follow-up test and confirmed that LPS curbed the viability and proliferation of

PDLCs and enhanced apoptosis and inflammatory response in a concentration-dependent manner.

Silencing circ_0099630 greatly mitigated the impacts of LPS on PDLCs

Circ_0099630 knockdown abated the promotion of LPS on circ_0099630, IL-6 and TNF-α level in PDLCs (Fig. 3A—C). In addition, the inhibitory effects of LPS on the viability and proliferation of PDLCs were recovered with the transfection of si-circ_0099630 (Fig. 3D and E). Meanwhile, LPS-enhanced apoptosis and the protein levels of Cleaved-caspase-3 and Bax were reversed after si-circ_0099630 was transfected into PDLCs (Fig. 3F—H). In conclusion, the negative effects of LPS on the function of PDLCs were mitigated by knockdown of circ_0099630.

Circ_0099630 sponged and downregulated miR-940

The complementary sequences of circ_0099630 and miR-940 predicted by Circinteractome were displayed in Fig. 4A.
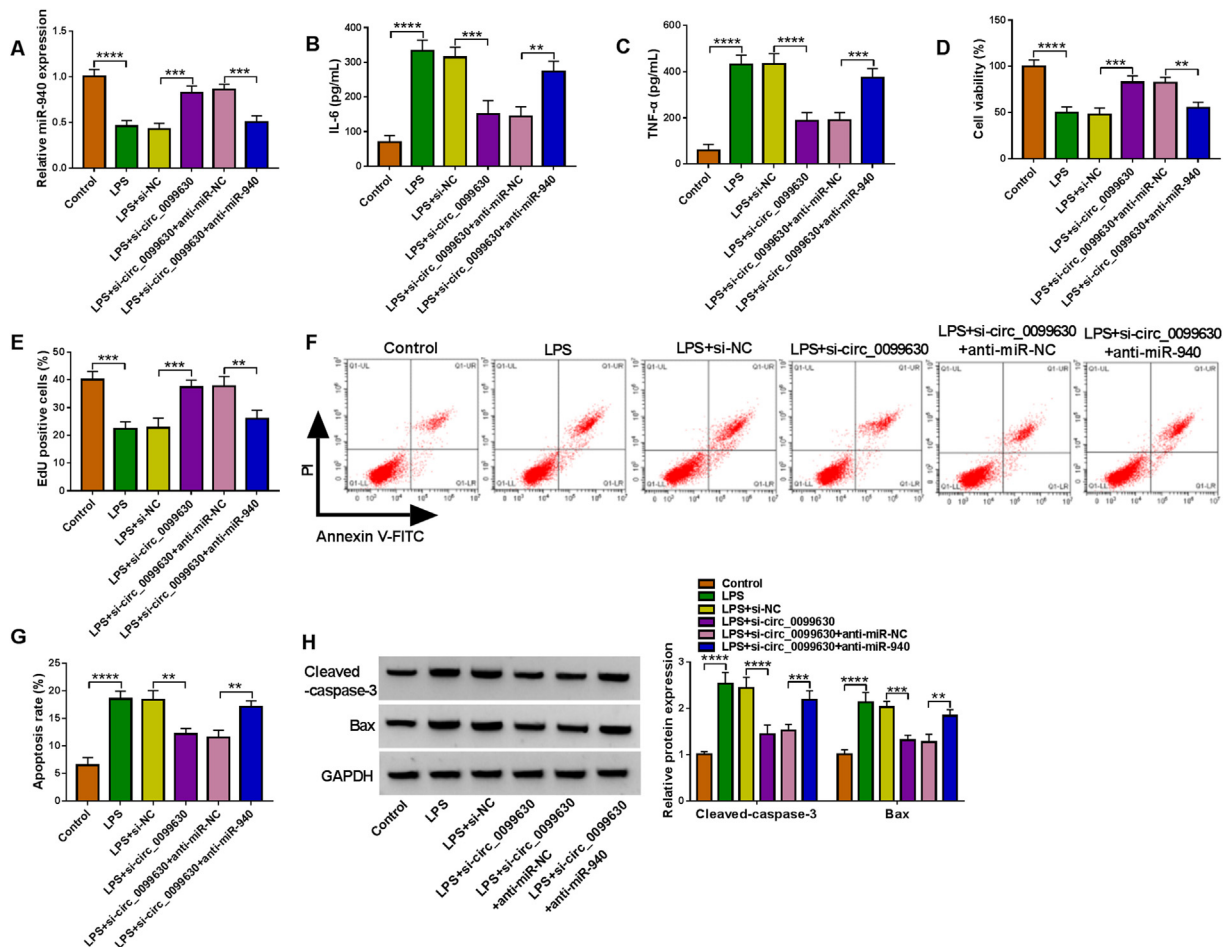

Figure 5 **MiR-940 and circ_0099630 jointly regulated the function of LPS-induced PDLCs.** (A—H) There were six groups which were Control, LPS, LPS + si-NC, LPS + si-circ_0099630, LPS + si-circ_0099630+anti-miR-NC, LPS + si-circ_0099630+anti-miR-940. (A) The implementation of qRT-PCR analyzed miR-940 level. (B and C) ELISA detected the IL-6 and TNF-α levels. (D) Cell viability was detected using CCK8 assay. (E) EdU assay was performed to detect proliferation. (F and G) The execution of flow cytometry determined apoptosis. (H) Cleaved-caspase-3 and Bax protein levels were measured by Western blot. **P < 0.01, ***P < 0.001, ****P < 0.001.

MiR-940 level was markedly enhanced with the introduction of miR-940 mimic in PDLCs (Fig. 4B). The luciferase activity in the WT-circ_0099630 group was greatly curbed by miR-940 mimic, however, no change appeared in the MUT-circ_0099630 group (Fig. 4C). Also, RIP assay also indicated that circ_0099630 and miR-940 were dramatically enriched in the Ago2 group relative to the IgG group, further supporting their targeting relationship (Fig. 4D). Next, low abundance of miR-940 was observed in periodontitis tissues and negatively correlated with circ_0099630 level (Fig. 4E and F). Additionally, the abundance of miR-940 was reduced in periodontitis tissues with the progression of the severity of periodontitis (Fig. 4E). Furthermore, we found that miR-940 level was decreased in PDLCs with increasing LPS concentration (Fig. 4G). The reciprocal relationship between circ_0099630 and miR-940 was evidenced by these data.

MiR-940 silencing alleviated the effects of circ_0099630 knockdown on LPS-induced PDLCs

The promotion of si-circ_0099630 on miR-940 level and the inhibition on IL-6 and TNF-α levels were diminished by co-transfection with anti-miR-940 in LPS-induced PDLCs (Fig. 5A−C). Si-circ_0099630-enhanced the impacts of cell

viability and proliferation were receded by silencing miR-940 in LPS-induced PDLCs (Fig. 5D and E). Meanwhile, anti-miR-940 mitigated si-circ_0099630-mediated suppression on apoptosis and Cleaved-caspase-3, Bax protein levels in LPS-induced PDLCs (Fig. 5F−H). Collectively, miR-940 and circ_0099630 jointly regulated the malignant behavior of LPS-induced PDLCs.

MiR-940 targeted and downregulated TRAF6

Targetscan software discovered the potential binding sites for miR-940 and TRAF6, as illustrated in Fig. 6A. Luciferase activity was greatly downregulated in the WT-TRAF6 3′UTR and miR-940 mimic co-transfection group, but no difference was observed in the MUT-TRAF6 3′UTR group (Fig. 6B), tentatively proving the relationship between miR-940 and TRAF6. The phenomenon that miR-940 and TRAF6 were heavily adsorbed in the Ago2 group further demonstrated the association between miR-940 and TRAF6 (Fig. 6C). High level of TRAF6 was found in periodontitis tissues compared to normal tissues and was negatively correlated with miR-940 level (Fig. 6D and E). Also, TRAF6 expression was significantly elevated in periodontitis tissues with the progression of the severity of periodontitis (Fig. 6D). The high abundance of TRAF6 in periodontitis tissues and LPS-induced PDLCs was
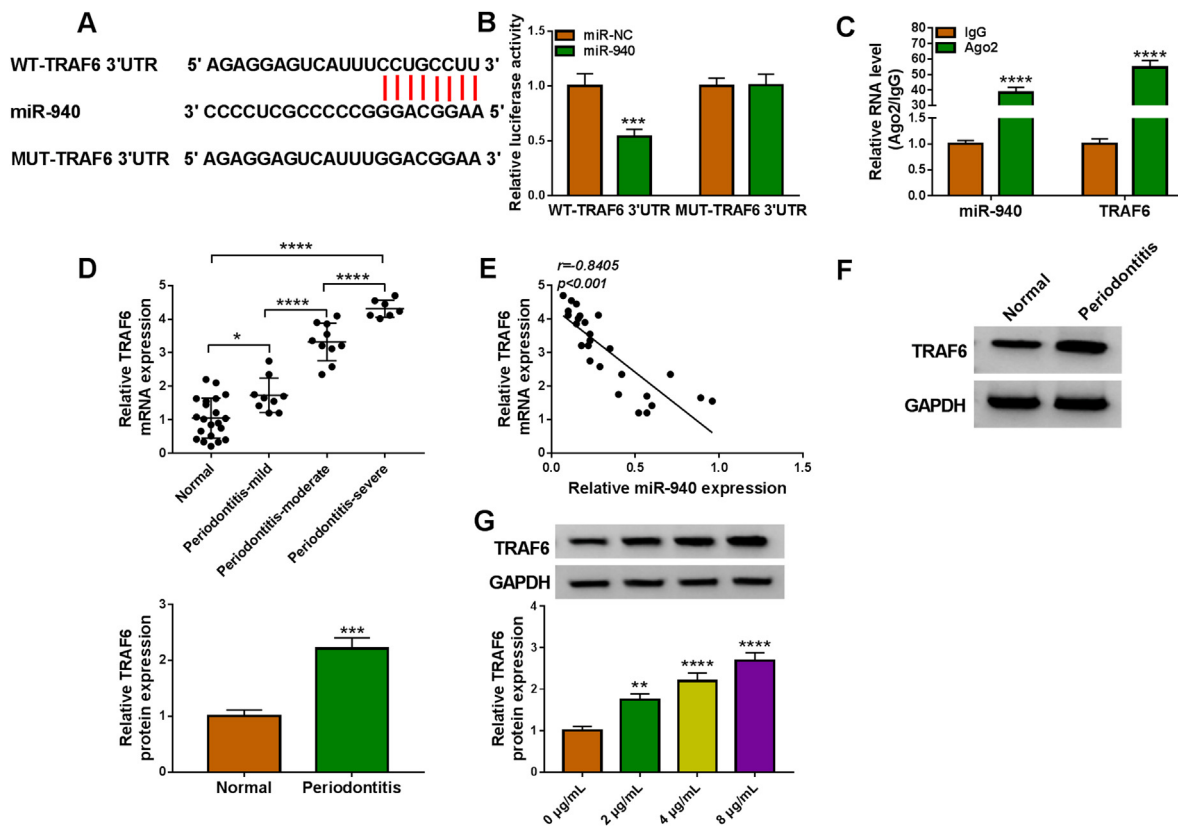

Figure 6 **The relationship between TRAF6 and miR-940 was validated.** (A) Binding sites of TRAF6 and miR-940. (B) The targeting relationship of TRAF6 and miR-940 was evidenced through dual-luciferase reporter system. (C) RIP assay proved the relationship of TRAF6 and miR-940. (D) TRAF6 content in periodontitis tissues was analyzed by qRT-PCR. (E) Correlation analysis of TRAF6 and miR-940 levels in periodontitis tissues was revealed using Pearson analysis. (F and G) Western blot measured TRAF6 protein level in periodontitis tissues and LPS-induced PDLCs. $*P < 0.05$, $**P < 0.01$, $***P < 0.001$, $****P < 0.001$.

also observed by Western blot results (Fig. 6F and G). TRAF6 was identified as a target of miR-940 by these results.

TRAF6 upregulation reverted the effects of miR-940 mimic on LPS-induced PDLCs

TRAF6 overexpression reinstated the downregulation of TRAF6 level induced by miR-940 mimic in LPS-induced PDLCs (Fig. 7A). The depressed effects of miR-940 upregulation on IL-6 and TNF-α levels were recuperated by TRAF6 overexpression in LPS-induced PDLCs (Fig. 7B and C). Enhancing effects of miR-940 mimic on the viability and proliferation of LPS-induced PDLCs were diminished with TRAF6 co-transfection (Fig. 7D and E). Besides, miR-940 upregulation impeded apoptosis and Cleaved-caspase-3 and Bax protein expression in LPS-induced PDLCs, but TRAF6 upregulation ameliorated this phenomenon (Fig. 7F–H). Also, we observed that miR-940 down-regulation mitigated the inhibition of TRAF6 protein level in LPS-induced PDLCs by si-circ_0099630 (Fig. 8A). Si-circ_0099630-repressed phosphorylation levels of P65 and IκBα in LPS-induced PDLCs were restored accompanied by co-transfection of anti-miR-940 or TRAF6 (Fig. 8B). These

illustrated that miR-940 silencing and TRAF6 overexpression activated the si-circ_0099630-suppressed NF-κB signaling pathway, which in turn facilitated the inflammatory response. Overall, LPS-induced PDLCs injury was co-regulated by circ_0099630/miR-940/TRAF6 axis.

Discussion

The inaccuracy of periodontitis diagnosis had accelerated the study of its molecular diagnostic markers.[26,27] LPS was used to stimulate the inflammatory conditions of periodontitis, and LPS-induced periodontitis *in vitro* and *in vivo* models had been widely used for investigation of the molecular mechanisms of periodontitis pathogenesis.[28-30] Our study validated the expression profile and action mechanism of circ_0099630/miR-940/TRAF6 axis in periodontitis tissues and model cells induced by LPS.

CircRNAs were more abundantly expressed in various types of tissues while being more stable, conditions that support their use as molecular markers for diagnosis and treatment of various diseases.[31] We observed a higher abundance of circ_0099630 in periodontitis tissues and model cells compared to normal tissues and cells, which
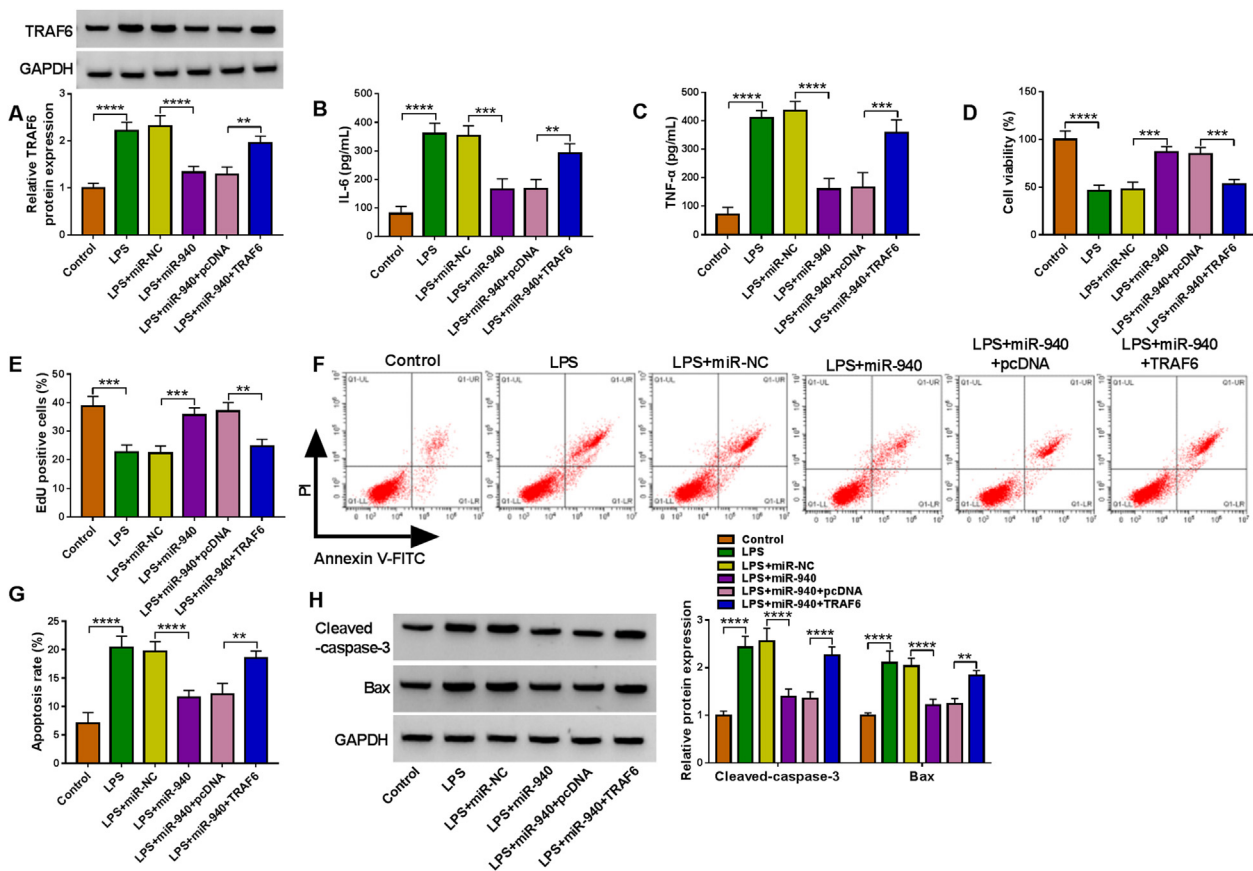

Figure 7 **LPS-induced PDLCs function was co-regulated by miR-940/TRAF6 axis.** (A–H) There were six groups, Control, LPS, LPS + miR-NC, LPS + miR-940, LPS + miR-940+pcDNA, LPS + miR-940+TRAF6. (A and B) IL-6 and TNF-α levels were measured through ELISA. (C and D) Cell viability and proliferation were detected after the performance of CCK8 and EdU assays. (F and G) Flow cytometry was executed to analyze the apoptosis. (H) Cleaved-caspase-3 and Bax protein levels were revealed in Western blot. **P < 0.01, ***P < 0.001, ****P < 0.001.
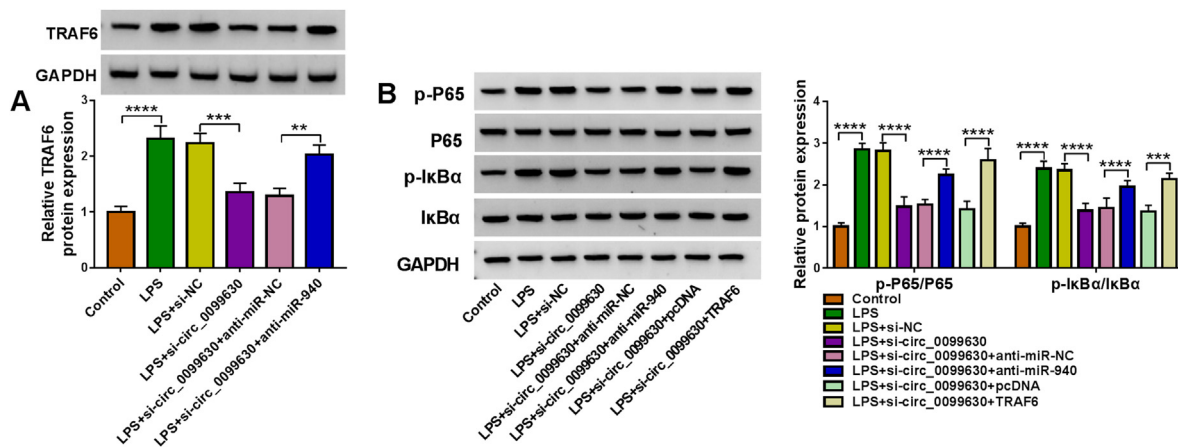
Figure 8 Circ_0099630 and miR-940 co-regulated the levels of TRAF6 and key molecules in the NF-κB pathway. (A) TRAF6 protein level was checked by Western blot. (B) Under the application of Western blot, the phosphorylation levels of P65 and IκBα were analyzed. **$P < 0.01$, ***$P < 0.001$, ****$P < 0.001$.

suggested that circ_0099630 was expected to be a more rapid and ready diagnostic marker for periodontitis in the future, and the analysis of the association between circ_0099630 level and clinical symptoms of periodontitis patients should be enhanced in the future. Consistent with our findings, Li et al. unveiled that circ_0138960 were greatly upregulated in periodontitis tissues.[12] We found after a series of validation that circ_0099630 knockdown effectively alleviated the inhibition of proliferation of PDLCs by LPS. In addition, IL-6 and TNF-α were identified as inflammatory markers,[32] and circ_0099630 knockdown also suppressed the cellular levels of IL-6 and TNF-α in LPS-induced PDLCs. All these data pointed to circ_0099630 as a very promising molecular target for the diagnosis and treatment of periodontitis in the future.

In this study, miR-940 was identified as a target of circ_0099630 to co-regulate LPS-induced injury in PDLCs. MiR-940 had established a critical role in human diseases. For example, miR-940 could enhance the progression of breast cancer and endometrial carcinoma.[19,33] MiR-940 might function as a protective factor in lung adenocarcinoma and esophageal squamous cell carcinoma.[21,34] Moreover, miR-940 participated in the inflammatory response of IL-1β-stimulated chondrocytes in a MyD88-dependent manner, indicating its regulation in osteoarthritis.[35] MiR-940 downregulation in periodontitis tissues and model cells was detected in the study. Meanwhile, miR-940 downregulation abrogated the mitigating effect of circ_0099630 knockdown on LPS-induced damage in PDLCs. Combined regulation of periodontitis process by circ_0099630 and miR-940 was confirmed in our study.

The targeting relationship between TRAF6 and miR-940 was established in this study, and TRAF6 had a high abundance in periodontitis tissues and model cells. In previous studies, TRAF6 was detected in higher abundance in tissues with myocardial hypertrophy.[36] Xie et al. identified that TRAF6 combined with miR-125/124 axis was involved in the regulation of the nuclear factor kappa-B (NF-κB) signaling pathway and chemoresistance.[37] The NF-κB signaling was an inflammation-associated signaling pathway.[38] In our study, the TRAF6/circ_0099630/miR-940 axis jointly regulated the phosphorylation levels of P65 and IκBα and thus participating in the regulation of NF-κB signaling pathway activation. Meanwhile, TRAF6 level was co-regulated by circ_0099630/miR-940 axis, and the circ_0099630/miR-940/TRAF6 axis jointly regulated periodontitis progression.

In conclusion, silencing circ_0099630 alleviated LPS-induced periodontal ligament cell injury via targeting miR-940/TRAF6/NF-κB axis in periodontitis, which provides a promising target for future diagnosis and treatment of periodontitis.

Declaration of competing interest

The authors have no conflicts of interest relevant to this article.

Appendix A. Supplementary data

Supplementary data to this article can be found online at https://doi.org/10.1016/j.jds.2022.04.005.

References

1. Slots J. Periodontitis: facts, fallacies and the future. *Periodontol 2000* 2017;75:7—23.
2. Contreras A, Moreno SM, Jaramillo A, et al. Periodontal microbiology in Latin America. *Periodontol 2000* 2015;67:58—86.
3. Botero JE, Vidal C, Contreras A, Parra B. Comparison of nested polymerase chain reaction (PCR), real-time PCR and viral culture for the detection of cytomegalovirus in subgingival samples. *Oral Microbiol Immunol* 2008;23:239—44.
4. Li X, Sun QF, Sun YD, Ge SH, Yang PS. Quantitative detection of human cytomegalovirus in aggressive and chronic periodontitis lesions. *Hua xi kou qiang yi xue za zhi* 2011;29:242—5.
5. Papapanou PN, Susin C. Periodontitis epidemiology: is periodontitis under-recognized, over-diagnosed, or both? *Periodontol 2000* 2017;75:45—51.

6. Krishna R, De Stefano JA. Ultrasonic vs. hand instrumentation in periodontal therapy: clinical outcomes. *Periodontol 2000* 2016;71:113—27.

7. Heitz-Mayfield LJ, Lang NP. Surgical and nonsurgical periodontal therapy. Learned and unlearned concepts. *Periodontol 2000* 2013;62:218—31.

8. Shi Y, Jia X, Xu J. The new function of circRNA: translation. *Clin Transl Oncol* 2020;22:2162—9.

9. Su Y, Lv X, Yin W, et al. CircRNA Cdr1as functions as a competitive endogenous RNA to promote hepatocellular carcinoma progression. *Aging (Albany NY)* 2019;11:8183—203.

10. Qi T, Zhang D, Shi X, Li M, Xu H. Decreased circUBAP2 expression is associated with preeclampsia by limiting trophoblast cell proliferation and migration. *Reprod Sci* 2021;28:2237—45.

11. Zhang J, Cheng F, Rong G, Tang Z, Gui B. Hsa_circ_0005567 activates autophagy and suppresses IL-1β-induced chondrocyte apoptosis by regulating miR-495. *Front Mol Biosci* 2020;7:216.

12. Li J, Xie R. Circular RNA expression profile in gingival tissues identifies circ_0062491 and circ_0095812 as potential treatment targets. *J Cell Biochem* 2019;120:14867—74.

13. Lu TX, Rothenberg ME. MicroRNA. *J Allergy Clin Immunol* 2018; 141:1202—7.

14. Correia de Sousa M, Gjorgjieva M, Dolicka D, Sobolewski C, Foti M. Deciphering miRNAs' action through miRNA editing. *Int J Mol Sci* 2019;20:6249.

15. Kessler D, Burns A, Tallon D, et al. Combining mirtazapine with SSRIs or SNRIs for treatment-resistant depression: the MIR RCT. *Health Technol Assess* 2018;22:1—136.

16. Wei Z, Chang K, Fan C, Zhang Y. MiR-26a/miR-26b represses tongue squamous cell carcinoma progression by targeting PAK1. *Cancer Cell Int* 2020;20:82.

17. Zhou W, Su L, Duan X, et al. MicroRNA-21 down-regulates inflammation and inhibits periodontitis. *Mol Immunol* 2018; 101:608—14.

18. Guo J, Zeng X, Miao J, et al. MiRNA-218 regulates osteoclast differentiation and inflammation response in periodontitis rats through Mmp9. *Cell Microbiol* 2019;21:e12979.

19. Zhang H, Peng J, Lai J, et al. MiR-940 promotes malignant progression of breast cancer by regulating FOXO3. *Biosci Rep* 2020;40. BSR20201337.

20. Wang B, Shen PF, Qu YX, et al. miR-940 promotes spinal cord injury recovery by inhibiting TLR4/NF-κB pathway-mediated inflammation. *Eur Rev Med Pharmacol Sci* 2019;23:3190—7.

21. Wang H, Song T, Qiao Y, Sun J. miR-940 inhibits cell proliferation and promotes apoptosis in esophageal squamous cell carcinoma cells and is associated with post-operative prognosis. *Exp Ther Med* 2020;19:833—40.

22. Dou Y, Tian X, Zhang J, Wang Z, Chen G. Roles of TRAF6 in central nervous system. *Curr Neuropharmacol* 2018;16:1306—13.

23. Ishida T, Mizushima S, Azuma S, et al. Identification of TRAF6, a novel tumor necrosis factor receptor-associated factor protein that mediates signaling from an amino-terminal domain of the CD40 cytoplasmic region. *J Biol Chem* 1996;271:28745—8.

24. Lee NK, Lee SY. Modulation of life and death by the tumor necrosis factor receptor-associated factors (TRAFs). *J Biochem Mol Biol* 2002;35:61—6.

25. Yuan P, Liu Z, Liu M, Huang J, Li X, Zhou X. Up-regulated tumor necrosis factor-associated factor 6 level is correlated with apoptosis in the rat cerebral ischemia and reperfusion. *Neurol Sci* 2013;34:1133—8.

26. Dannewitz B, Holtfreter B, Eickholz P. Periodontitis-therapy of a widespread disease. *Bundesgesundheitsblatt - Gesundheitsforsch - Gesundheitsschutz* 2021;64:931—40.

27. Kwon T, Lamster IB, Levin L. Current concepts in the management of periodontitis. *Int Dent J* 2021;71:462—76.

28. Zheng Y, Dong C, Yang J, et al. Exosomal microRNA-155-5p from PDLSCs regulated Th17/Treg balance by targeting sirtuin-1 in chronic periodontitis. *J Cell Physiol* 2019;234: 20662—74.

29. Huang N, Li C, Sun W, Wu J, Xiao F. Long non-coding RNA TUG1 participates in LPS-induced periodontitis by regulating miR-498/RORA pathway. *Oral Dis* 2021;27:600—10.

30. Li Y, Lu Z, Zhang L, Kirkwood KL, Lopes-Virella MF, Huang Y. Acid sphingomyelinase deficiency exacerbates LPS-induced experimental periodontitis. *Oral Dis* 2020;26:637—46.

31. Wang Y, Li Z, Xu S, Guo J. Novel potential tumor biomarkers: circular RNAs and exosomal circular RNAs in gastrointestinal malignancies. *J Clin Lab Anal* 2020;34:e23359.

32. Zhang J, Chi H, Xiao H, et al. Interleukin 6 (IL-6) and tumor necrosis factor α (TNF-α) single nucleotide polymorphisms (SNPs), inflammation and metabolism in gestational diabetes mellitus in inner Mongolia. *Med Sci Mon Int Med J Exp Clin Res* 2017;23:4149—57.

33. Zhou Z, Xu YP, Wang LJ, Kong Y. miR-940 potentially promotes proliferation and metastasis of endometrial carcinoma through regulation of MRVI1. *Biosci Rep* 2019;39. BSR20190077.

34. Ma Q, Zhang J, Huang J, et al. Decreased miR-940 expression can predict a negative prognosis in early-stage nonsmoking female lung adenocarcinoma. *Transl Lung Cancer Res* 2021;10: 4293—302.

35. Cao J, Liu Z, Zhang L, Li J. miR-940 regulates the inflammatory response of chondrocytes by targeting MyD88 in osteoarthritis. *Mol Cell Biochem* 2019;461:183—93.

36. Ji YX, Zhang P, Zhang XJ, et al. The ubiquitin E3 ligase TRAF6 exacerbates pathological cardiac hypertrophy via TAK1-dependent signalling. *Nat Commun* 2016;7:11267.

37. Sun J, Wang J, Lu W, et al. MiR-325-3p inhibits renal inflammation and fibrosis by targeting CCL19 in diabetic nephropathy. *Clin Exp Pharmacol Physiol* 2020;47:1850—60.

38. Lawrence T. The nuclear factor NF-kappaB pathway in inflammation. *Cold Spring Harbor Perspect Biol* 2009;1: a001651.